Impact of Mutual Coupling and Antenna Efficiencies on Adaptive Switching Between MIMO Transmission Strategies

R. Bhagavatula[†], R. W. Heath Jr.[†], A. Forenza[♯], D. Piazza[‡] and K. R. Dandekar[‡]
[†] The University of Texas at Austin, Austin, Texas
{bhagavat, rheath}@ece.utexas.edu
[♯] Rearden, LLC, San Francisco, California
antonio@rearden.com
[‡] Drexel University, Philadelphia, Pennsylvania
dp84@drexel.edu,dandekar@ece.drexel.edu

***Abstract*— Previous research has shown that adaptive switching between multiple-input multiple-output (MIMO) transmission strategies like spatial multiplexing and beamforming increases link reliability and capacity gains, as compared to fixed transmission strategies. To get the full benefit of adaptive switching it is necessary to obtain accurate estimates of the SNR values when we switch between the transmission strategies. In this paper, it is shown that (relatively more) accurate switching point estimates can be obtained by taking into account real-life effects like mutual coupling and antenna efficiencies, for switching between statistical beamforming and spatial multiplexing. Using simulations, it is shown that accounting for these effects can make the switching point estimate more accurate by as much as 12 dB, compared to the case when the practical effects are not considered.**

I. Introduction

Multiple-input multiple-output (MIMO) systems employ multiple antennas at the transmitter and receiver. MIMO wireless technology can provide much higher data rates and link robustness as compared to a single-input single-output system [1], using a variety of transmission strategies like spatial multiplexing (SM) [2] - [4] and diversity techniques like beamforming [5], [6]. The performance of a MIMO communication link can be approximated by its ergodic capacity, when good coding techniques are used [7]. A practical means of approaching the spatially-correlated MIMO channel capacity is to use statistical switching between low complexity schemes like statistical beamforming and spatial multiplexing. The transmitter switches between different transmission strategies in response to varying channel conditions [8] - [10].

In our paper, we analyze adaptive switching between SM and statistical beamforming (SBF) [6]. Adaptive switching can occur using both, instantaneous channel information [9] (requiring a large amount of feedback), or using statistical information about the spatial correlation matrices, as in [10]. We use correlation matrices in this paper, as spatial correlation matrices play a dominant role in determining the optimal transmit strategy, vary slowly as compared to instantaneous channel state and hence, offer an effective tradeoff between performance and feedback requirements.

The performance gains made possible by adaptive switching cannot be realized if the switching point estimates are not accurate, i.e. if the switching between SBF and SM occurs much before or much after the intended point, the performance gains obtained will be lesser than desired. To get (relatively more) accurate switching point estimates, it is necessary to include practical effects like mutual coupling (MC) and antenna efficiencies (AE)[1] in the evaluation of the ergodic capacities of the two transmission strategies and the switching points between them. While there has been work done previously to analyze the impact of MC on the capacity of a MIMO channel [11] - [15], there has been no attempt to explore the impact of MC and AE on adaptive switching between MIMO transmission strategies. Also, all previous work on adaptive switching assumes unit antenna efficiencies. This is not accurate, as practical antennas can have efficiencies as low as 50% - 60% on account of ohmic, coupling, and dielectric losses.

In this paper, we show that it is necessary to account for the impact of MC and AE to obtain more accurate estimates of the switching points between SBF and SM. We first derive expressions for the ergodic capacity of SBF and SM. Using these expressions, we show that more accurate capacity gain estimates can be obtained if we include MC and AE effects in the evaluation of ergodic capacities. We then derive switching point estimates based on the upper bounds of the ergodic capacities of the two strategies and show that there can be a difference of as much as 12 dB in the switching points if we do not account for these effects.

II. System Description and Performance Evaluation

Consider a MIMO system with M_T transmit and M_R receive antennas. Assuming a block time-invariant channel, the discrete-time input-output relation of the MIMO system (the discrete time index has been dropped for the sake of convenience) is given by

$$\mathbf{y} = \sqrt{\frac{E_s}{M_T}}\mathbf{H}\mathbf{s} + \mathbf{n} \tag{1}$$

[1] Antenna efficiency is the ratio of the power radiated by an antenna to the power into the antenna.

1-4244-0264-6/07/$25.00 ©2007 IEEE

where $\mathbf{y} \in \mathbb{C}^{M_R \times 1}$ is the received signal, $\mathbf{s} \in \mathbb{C}^{M_T \times 1}$ is the transmit signal constrained such that its covariance matrix, $\mathbf{R_{ss}} = \mathcal{E}\{\mathbf{ss}^\dagger\}$[2], satisfies $\mathrm{Tr}(\mathbf{R_{ss}}) = M_T$ and E_s is the total average energy available at the transmitter over a symbol period. The MIMO channel transfer matrix is denoted by $\mathbf{H} \in \mathbb{C}^{M_R \times M_T}$, and $\mathbf{n} \in \mathbb{C}^{M_R \times 1}$ is the complex additive white Gaussian noise at the receive antennas, with $\mathcal{E}\{\mathbf{nn}^\dagger\} = N_o \mathbf{I}_{M_R}$.

For our analysis, we use the Kronecker model [16], [17], in which the channel transfer matrix is given by

$$\mathbf{H} = \mathbf{R}_r^{1/2} \mathbf{H}_w \mathbf{R}_t^{1/2} \tag{2}$$

where $\mathbf{R}_t$ and $\mathbf{R}_r$ denote the transmit and receive spatial correlation matrices, respectively, and $\mathbf{H}_w \in \mathbb{C}^{M_R \times M_T}$, is a matrix of independent complex i.i.d. Gaussian entries with zero mean and unit variance. The channel matrix, $\mathbf{H}$, is normalized so that $\mathcal{E}\{\|\mathbf{H}\|_F^2\} = M_T M_R$. In the presence of a large amount of correlation, it has been shown in [18] that the capacity predicted by the Kronencker model is lower than the measured capacity and does not describe the multipath structure of the channel accurately. In this paper, however, we prefer to use the Kronecker model due to its analytical tractability.

We use the clustered channel model [19] for our analysis. It is shown in [20] that channel models disregarding cluster effects overestimate channel capacity. The clustered model has also been validated through measurements [21], [22] and variations have been used for different standards like IEEE 802.11n Technical Group [23] and the 3GPP Technical Specification Group [24] for system design and evaluation of cellular systems.

III. Antenna Configurations and Setup

In this paper, we use one of the antenna configurations described in [25]. The reconfigurable antenna array in [25] consists of two reconfigurable microstrip dipoles designed to resonate at a frequency of 2.45 GHz. Each dipole-arm is made of two metallic strips laid out lengthwise and connected by a PIN diode switch [25]. The first strip, $\lambda_r/2$ in length (λ_r is the wavelength at the resonant frequency) is connected to the feed network. When the PIN diode is turned off, the strips are electrically isolated and only the first strip radiates. Upon turning on the PIN diode, the second strip is electrically connected to the first thus forming a longer radiating arm of $3\lambda_r/4$ length. The two PIN diodes within the antenna operate synchronously. Thus each dipole antenna can be configured to have two configurations: 'short' when the switches are turned off and 'long' when the switches are turned on. For our analysis, we consider only the 'long-long' configuration, with an antenna efficiency of 62%. The antennas are separated by a distance of $\lambda_r/4$. Fig. 1 shows the gain pattern of the long-long array configuration. The effect of mutual coupling can be seen by comparing these array patterns with that of a single antenna pattern shown in Fig. 1. The S-parameters for the 'long-long' configuration were measured with a calibrated Agilent N5230A Network Analyzer. Antenna efficiencies were calculated using the electromagnetic software, FEKO [26], that takes into consideration the ohmic, coupling, and dielectric losses of an antenna. The S-matrix of the long-long configuration in [25] is given as

$$\mathbf{S} = \begin{bmatrix} -4.3\angle -43.0^o & -16.1\angle -12.1^o \\ -16.4\angle -12.2^o & -5.4\angle -48.9^o \end{bmatrix}$$

where the magnitude is in dB and the angle is expressed in degrees.

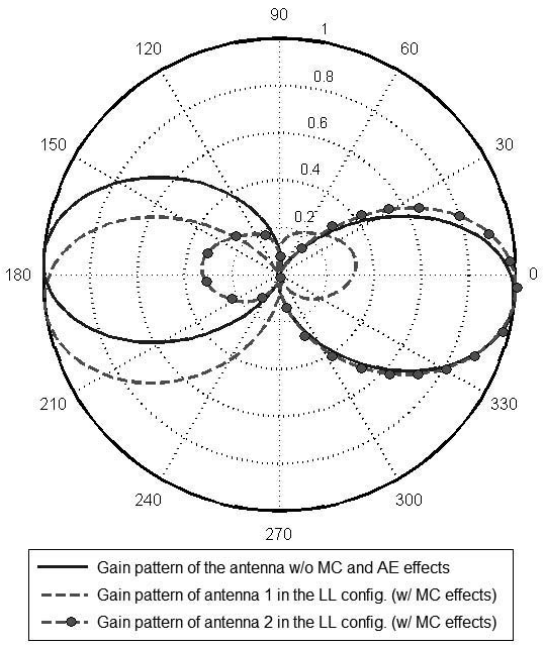

Fig. 1. Radiation patterns of the long-long configuration. The distortion induced by MC is evident in the pattern.

IV. Evaluation of Ergodic Capacity, Including MC and AE

Let $\mathbf{S}_T \in \mathbb{C}^{M_T \times M_T}$ and $\mathbf{S}_R \in \mathbb{C}^{M_R \times M_R}$ represent the mutual coupling matrices at the transmit and receive sides respectively. Also, let Δ_T and Δ_R stand for the transmit and receive antenna array efficiencies respectively. To incorporate the MC effects into the evaluation of ergodic capacity, we represent the effective channel matrix by [27]

$$\mathbf{H}_{\text{eff}} = (\mathbf{I}_{M_R} - \mathbf{S}_R)\mathbf{H}(\mathbf{I}_{M_T} - \mathbf{S}_T) \ . \tag{3}$$

From (2) and (3), we include the effect of antenna efficiencies into the expression to give

$$\mathbf{H}_{\text{eff}} = (\mathbf{I}_{M_R} - \mathbf{S}_R)(\Delta_R \mathbf{R}_r)^{1/2} \mathbf{H}_w (\Delta_T \mathbf{R}_t)^{1/2} (\mathbf{I}_{M_T} - \mathbf{S}_T) \ . \tag{4}$$

Note that $\mathbf{R}_t$ and $\mathbf{R}_r$ in (4) accounts for the antenna radiation patterns in Fig. 1, according to the definition of spatial correlation in [28], [29]. Hence, (4) accounts for all three

[2]In this paper, $\mathbf{X}$ refers to a matrix of the specified size. The transpose and Hermitian transpose of $\mathbf{X}$ is given by $\mathbf{X}^T$, and $\mathbf{X}^\dagger$ respectively. An identity matrix of size R is denoted by $\mathbf{I}_R$. Also, $\mathrm{Tr}(\mathbf{Y})$ and $|\mathbf{Y}|$ refer to the trace and determinant of a square matrix $\mathbf{Y}$, respectively. $\mathcal{E}\{.\}$ refers to the ergodic mean and $\|\mathbf{Y}\|_F$ stands for the Frobenius norm of $\mathbf{Y}$.

effects: MC, AE and pattern distortion. The coupling matrices are given by $\mathbf{C}_T = (\mathbf{I}_{M_T} - \mathbf{S}_T)$ and $\mathbf{C}_R = (\mathbf{I}_{M_R} - \mathbf{S}_R)$. When there is no mutual coupling on the transmit and receive antenna sides (when the antennas are placed far enough) and when the antennas on both sides have 100% efficiency, then $\mathbf{H}_{\text{eff}} = \mathbf{R}_r^{1/2}\mathbf{H}_w\mathbf{R}_t^{1/2}$, as shown in (2).

We now show how MC and AE effects can be incorporated into the ergodic capacity expressions for a MIMO channel. The ergodic capacity of a MIMO channel is given by

$$C = \max_{\substack{\mathbf{R_{ss}} \\ \text{Tr}(\mathbf{R_{ss}})=E_s}} \mathcal{E}\left\{\log_2\left|\mathbf{I}_{M_R} + \frac{1}{N_o}\mathbf{H}\mathbf{R_{ss}}\mathbf{H}^\dagger\right|\right\}\frac{\text{b/s}}{\text{Hz}}\ . \quad (5)$$

To incorporate the effect of mutual coupling in (5), we replace $\mathbf{H}$ by $\mathbf{H}_{\text{eff}}$ (from (4)) to give

$$C = \max_{\substack{\mathbf{R_{ss}} \\ \text{Tr}(\mathbf{R_{ss}})=E_s}} \mathcal{E}\left\{\log_2\left|\mathbf{I}_{M_R} + \frac{1}{N_o}\mathbf{H}_{\text{eff}}\mathbf{R_{ss}}\mathbf{H}_{\text{eff}}^\dagger\right|\right\}\frac{\text{b/s}}{\text{Hz}}\ . \quad (6)$$

To make our analysis tractable, we consider only single-sided correlation at the transmit side and unit efficiencies and zero MC at the receiver, i.e. we let $\mathbf{S}_R = \mathbf{0}$, $\Delta_R = 1$ and $\mathbf{R}_r = \mathbf{I}_{M_R}$. We also assume that $M_T = M_R = M$ for simplicity.

A. Capacity of MIMO System Using SBF, Including MC and AE

Due to the assumption of single-sided correlation at the transmitter, unit AE and zero MC at the receiver, we consider only the transmit side spatial correlation, AE and S-matrices. Let the eigenvalue decomposition of the Hermitian transmit covariance matrix, $\mathbf{R}_t = \mathbf{U}_T\Lambda_T\mathbf{U}_T^\dagger$. Similarly, we have $\mathbf{C}_T = \mathbf{U}_{C_T}\Lambda_{C_T}\mathbf{U}_{C_T}^\dagger$. In SBF, since all the data is transmitted over the strongest channel, the transmit signal covariance matrix, $\mathbf{R_{ss}}$ can be written as $\mathbf{R_{ss}}^{BF} = \mathbf{U}_{R_{ss}}^{BF}\Lambda_{R_{ss}}^{BF}(\mathbf{U}_{R_{ss}}^{BF})^\dagger$, where $\Lambda_{R_{ss}}^{BF} = \text{diag}\{E_s, 0, 0, \ldots\}$. We associate the first column of $\mathbf{U}_{R_{ss}}^{BF}$ to correspond to the largest eigenvalue of the channel. Similarly, the first eigenvalues in the matrices Λ_{C_T} and Λ_T, correspond to the largest eigenvalues denoted by $\lambda_{C_T}^{\max}$ and $\lambda_T^{\max}$ respectively. For the case of single sided correlation at the transmit side, unit AE and zero MC at the receive side, the ergodic capacity using SBF is obtained from (6) as

$$\begin{aligned} C_{\text{SBF}} &= \mathcal{E}\left\{\log_2\left|\mathbf{I}_M + \frac{1}{N_o}\mathbf{H}_{\text{eff}}\mathbf{R_{ss}}\mathbf{H}_{\text{eff}}^\dagger\right|\right\} \\ &= \mathcal{E}\left\{\log_2\left|\mathbf{I}_M + \frac{\Delta_T}{N_o}\mathbf{H}_w\mathbf{R}_t^{1/2}\mathbf{C}_T\mathbf{R_{ss}}\mathbf{C}_T^\dagger\mathbf{R}_t^{\dagger/2}\mathbf{H}_w^\dagger\right|\right\} \end{aligned} \quad (7)$$

where (7) is obtained from (4) by letting $\mathbf{R}_r = \mathbf{I}_M$, $\Delta_R = 1$ and $\mathbf{C}_R = \mathbf{I}_M$. Simplifying (7) using the eigenvalue decompositions of $\mathbf{R}_t$, $\mathbf{C}_T$ and $\mathbf{R_{ss}}$, and the matrix property $|\mathbf{I}_M + \mathbf{AB}| = |\mathbf{I}_M + \mathbf{BA}|$,

$$\begin{aligned} C_{\text{SBF}} &= \mathcal{E}\left\{\log_2\left|\mathbf{I}_M + \frac{E_s\Delta_T}{N_o}(\lambda_{C_T}^{\max})^2\lambda_T^{\max}\tilde{\mathbf{z}}\tilde{\mathbf{z}}^\dagger\right|\right\} \\ &= \mathcal{E}\left\{\log_2(1 + \rho\Delta_T(\lambda_{C_T}^{\max})^2\lambda_T^{\max}\tilde{\mathbf{z}}^\dagger\tilde{\mathbf{z}})\right\}\frac{\text{b/s}}{\text{Hz}} \end{aligned} \quad (8)$$

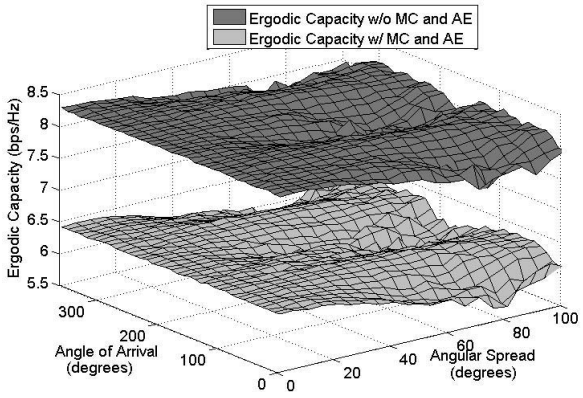

Fig. 2. Comparison of the ergodic capacities obtained for different angle of arrival and angular spread combinations, using statistical beamforming, for SNR = 20 dB.

where $\tilde{\mathbf{z}} = [z_1, z_2, \ldots, z_{M_R}]^T$. Here, z_i is a complex Gaussian random variable with zero mean and unit variance. Note that $\rho = E_s/N_o$. For the special case of zero MC and unit AE at the transmit side, $\lambda_{C_T}^{\max} = \Delta_T = 1$, reducing (8) to the expression in [10].

We now proceed to show the impact of MC and AE on the ergodic capacity of a MIMO system using SBF. Fig. 2 compares the ergodic capacities obtained when MC and AE are accounted for and when they are not, for different angles of arrival and angular spreads. We use the long-long configuration described in Section III for the simulations. From the figure, it is seen that the difference in the two values of ergodic capacities can be as much as 3 bps/Hz. This shows that not considering the impact of MC and AE in the evaluation of the ergodic capacity obtained using SBF can significantly overestimate the capacity gains. Hence, to get a (relatively more) accurate estimate of the capacity gains achievable using SBF, it is necessary to account for MC and AE effects.

The switching point between the SBF and SM is found using the upper bounds on the ergodic capacities of the same (to obtain a closed form simplified expression of the switching point). The upper bound for the ergodic capacity of a MIMO system employing SBF, including MC and AE, can be obtained from (8) as

$$\begin{aligned} C_{\text{SBF}} &\leq \log_2(1 + \rho\Delta_T(\lambda_{C_T}^{\max})^2\lambda_T^{\max}\mathcal{E}\{\tilde{\mathbf{z}}^\dagger\tilde{\mathbf{z}}\}) \quad (9) \\ &= \log_2(1 + \rho(\lambda_{C_T}^{\max})^2\lambda_T^{\max}M_R)\frac{\text{b/s}}{\text{Hz}} \quad (10) \end{aligned}$$

where (9) is obtained from Jensen's inequality, and from the fact that $\Delta_T(\lambda_{C_T}^{\max})^2\lambda_T^{\max}$ is a constant. For the special case of no mutual coupling, (10) reduces to the upper bound obtained in [10].

B. Capacity of MIMO System Using Spatial Multiplexing, Including MC and AE

We follow the derivation in [10] to obtain the ergodic capacity of a MIMO system using SM. We modify the derivation in [10] to include MC and AE effects. For SM with linear

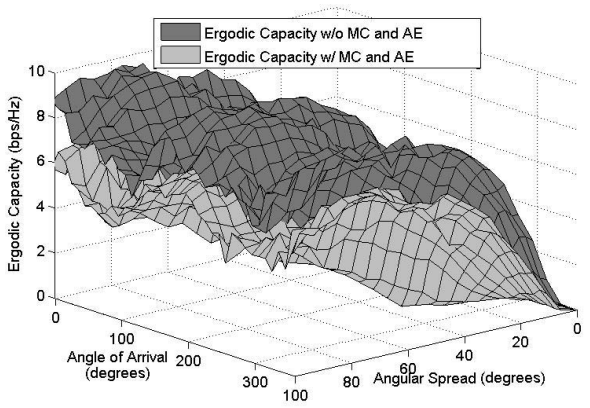

Fig. 3. Comparison of the ergodic capacities obtained for different angle of arrival and angular spread combinations, using spatial multiplexing, for SNR = 20 dB.

receivers, the MIMO channel is decoupled into $M_T(=M)$ parallel streams [30]. The conditional post-processing SNR for the k^{th} stream for a zero-forcing (ZF) receiver, ρ_k, is given by

$$\rho_k = \frac{\rho}{M_T} \frac{1}{\left[(\mathbf{H}_{\text{eff}}^{\dagger}\mathbf{H}_{\text{eff}})^{-1}\right]_{k,k}} \tag{11}$$

where $\mathbf{H}_{\text{eff}}$ is given by (4) and $[.]_{k,k}$ denotes the k^{th} diagonal element. To make our analysis tractable, we make the assumption of single sided correlation at the transmit side, unit AE and zero MC at the receive side, i.e. $(\mathbf{I}_{M_R} - \mathbf{S}_R)(\Delta_R\mathbf{R}_r)^{1/2} = \mathbf{I}_{M_R}$. We denote $(\Delta_T\mathbf{R}_t)^{1/2}(\mathbf{I}_{M_T} - \mathbf{S}_T) = (\widetilde{\mathbf{R}}_t)^{1/2}$. Then, from [10], the ergodic capacity of a MIMO system employing SM using a ZF receiver, including MC and AE effects, can be estimated as

$$C_{\text{SM}} = \sum_{k=1}^{M} \frac{\mathrm{e}^{\left(\frac{|\widetilde{\mathbf{R}}_t^{kk}|M_T}{|\widetilde{\mathbf{R}}_t|\rho}\right)}}{\ln 2} \Gamma\left(0, \frac{|\widetilde{\mathbf{R}}_t^{kk}|M_T}{|\widetilde{\mathbf{R}}_t|\rho}\right) \tag{12}$$

where $\widetilde{\mathbf{R}}_t^{kk}$ corresponds to $\widetilde{\mathbf{R}}_t$ with the k^{th} row and column removed and $\Gamma(.,.)$ is the incomplete Gamma function.

Fig. 3 compares the two cases when we include MC and AE in evaluating the ergodic capacity of a MIMO system using SM and when we do not, for the long-long array configuration described in Section III at SNR = 20 dB. The difference in the two values of ergodic capacities is as much as 4.5 bps/Hz. This difference in ergodic capacities is greater in the case of SM as compared to SBF. This is because in the case of SM, we use all the eigenvalues of the effective channel, whereas for SBF, we use only the largest eigenvalue. Hence, it is evident that accounting for MC and AE is important to obtain realistic estimates of the capacity gains that can be obtained using SM.

An upper bound of the capacity of SM with ZF receivers, including MC and AE effects, can be obtained from [10] to be

$$\begin{aligned} C_{\text{SM}} &\leq \log_2\left(1 + \sum_{k=1}^{M}(\rho\Delta_T)^k \left(\frac{1}{M_T}|\widetilde{\mathbf{R}}_t|\right)^k \text{tr}_k(\mathbf{A})\right) \\ &= \log_2\left(1 + \sum_{k=1}^{M}(\rho|\mathbf{C}_T|)^k \left(\frac{1}{M_T}|\mathbf{R}_t|\right)^k \text{tr}_k(\mathbf{A})\right) \end{aligned} \tag{13}$$

where $\mathbf{A} = \text{diag}(1/|\widetilde{\mathbf{R}}_t^{11}|, \ldots, 1/|\widetilde{\mathbf{R}}_t^{M_TM_T}|)$ and $\text{tr}_k(.)$ denotes the k^{th} elementary symmetric function (e.s.f.), defined as

$$\text{tr}_k(\mathbf{X}) = \sum_{\underline{\alpha}} \prod_{i=1}^{k} \lambda_{x,\alpha_i} = \sum_{\underline{\alpha}} |\mathbf{X}_{\underline{\alpha}}^{\underline{\alpha}}| \tag{14}$$

for arbitrary Hermitian positive-definite $\mathbf{X} \in \mathbb{C}^{n\times n}$. In (14), the sum is over all ordered $\underline{\alpha} = \{\alpha_1, \ldots \alpha_k\} \subseteq \{1, \ldots, n\}$, $\lambda_{x,i}$ denotes the i^{th} eigenvalue of $\mathbf{X}$, and $\mathbf{X}_{\underline{\alpha}}^{\underline{\alpha}}$ is the $k \times k$ principle submatrix of $\mathbf{X}$ formed by taking only the rows and columns indexed by $\underline{\alpha}$ [10].

C. Adaptive Switching Between SBF and SM, Including MC and AE

We use the ergodic capacity upper bounds from Sections IV-A and IV-B to obtain closed-form expressions for the switching points between SBF and SM, including mutual coupling and antenna efficiency effects. As in the previous section, we consider single-sided correlation at the transmitter, unit AE and zero MC at the receiver.

The switching point between SBF and SM, ρ_{CP} is the positive root of the expression obtained by equating the upper bounds for both the cases ((10) and (13)), as per

$$\sum_{k=1}^{M} \rho_{\text{CP}}^{k-1} \left(\frac{1}{M_T}|\widetilde{\mathbf{R}}_t|\right)^k \text{tr}_k(\mathbf{A}) - (\lambda_{C_T}^{\max})^2 \lambda_T^{\max} M_R = 0 \ . \tag{15}$$

For $M_T = M_R = 2$, (15) can be simplified to

$$\rho_{\text{CP}} = \frac{4(\lambda_{C_T}^{\max})^2\lambda_T^{\max} - |\widetilde{\mathbf{R}}_t|\text{tr}_1(\mathbf{A})}{\frac{1}{2}|\widetilde{\mathbf{R}}_t|^2\text{tr}_2(\mathbf{A})} \ . \tag{16}$$

To illustrate our results, we consider the long-long configuration described in the previous section. Fig. 4 shows the variation of switching points (from (16)) over a range of angles of arrival and angular spreads, when we take into account MC and AE effects and when we do not for SNR = 20 dB. Some of the switching points, particularly those for small angular spreads, are very high. This implies that for all practical conditions, SBF will outperform SM and hence, no switching will take place. The difference in switching points as seen from the plot is as large as 18 dB for an angle of arrival (AoA) of 90° and an angular spread (AS) of 10°. At more practical SNR regimes, the difference in switching point values include 11.53 dB for AS = 75° and AoA = 350°, 7.22 dB for AS = 75° and AoA = 190° and 7.19 dB for AS = 45°, AoA = 110°, etc. As Fig. 4 shows, we can obtain significantly more accurate estimates of the switching points between SBF and SM for a fixed configuration, if we consider the impact of mutual coupling and antenna efficiencies.

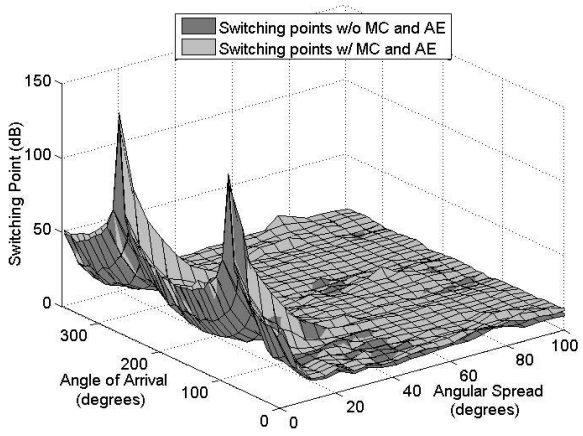

Fig. 4. Comparison of the switching points between SBF and SM for the long-long configuration, for different angle of arrival and angular spread combinations at SNR = 20 dB.

V. Conclusion

In this paper, we showed using antenna measurements, that it is necessary to incorporate mutual coupling and antenna efficiency effects when evaluating the capacity gains that can be obtained using MIMO transmission schemes like statistical beamforming and spatial multiplexing. We also showed that significantly more accurate estimates (up to 12 dB more accurate for reasonable SNR regimes) of the switching point between these two transmission schemes can be obtained by taking into account the mutual coupling between antenna elements and the antenna efficiencies. We conclude that accounting for mutual coupling and antenna efficiency effects when evaluating capacity gains, or switching points for adaptively switching between transmission strategies will improve the accuracy of the estimates significantly.

References

[1] G. J. Foschini, and M. J. Gans, "On Limits of Wireless Communications in a Fading Environment When Using Multiple Antennas," *Wireless Pers. Comm.*, vol. 6, no. 3, pp. 311 - 335, Mar. 1998.

[2] G. J. Foschini, "Layered Space-Time Architecture for Wireless Communications in a Fading Environment when Using Multiple Antennas", *Bell Labs Tech. Jrnl.*, vol. 1, no. 2, pp. 41 - 59, 1996.

[3] G. D. Golden, G. J. Foschini, R. A. Valenzuela and P. W. Wolniansky, "Detection Algorithm and Initial Laboratory Results using the V-BLAST Space-Time Communications Architecture," *IEEE Elec. Letters*, vol. 35, no. 7, pp. 14 - 15, Jan. 1999.

[4] A. J. Paulraj and T. Kailath, "Increasing Capacity in Wireless Broadcast Systems Using Distributed Transmission/Directional Reception (DTDR)," U. S. Patent 5,345,599, Sep. 1994.

[5] E. A. Jorswieck and H. Boche, "Channel capacity and capacity-range of beamforming in MIMO wireless systems under correlated fading with covariance feedback," *IEEE on Trans. Wireless Comm.*, vol. 3, pp. 1543 - 1553, Sep. 2004.

[6] M. Kang and M. S. Alouini, "Water-Filling Capacity and Beamforming Performance of MIMO Systems with Covariance Feedback," *IEEE Work. on Sign. Proc. Adv. in Wireless Comm.*, pp. 556 560, June 2003.

[7] D. S. Shiu, G. J. Foschini, M. J. Gans and J. M. Kahn, "Fading Correlation and its Effect on the Capacity of Multielement Antenna Systems," *IEEE Trans. on Comm.*, vol. 48, no. 3, pp. 502 513, Mar. 2000.

[8] D. Gesbert, M. Shafi, D. Shiu, P. J. Smith and A. Naguib, "From Theory to Practice: An Overview of MIMO SpaceTime Coded Wireless Systems," *IEEE Jrnl. on Select. Areas of Comm.*, vol. 21, no. 3, pp. 281 - 302, Apr. 2003.

[9] R. W. Heath, Jr. and A. J. Paulraj, "Switching Between Diversity and Multiplexing in MIMO Systems," *IEEE Trans. on Comm.*, vol. 53, no. 6, pp. 962 - 968, June 2005.

[10] A. Forenza, M. R. McKay, A. Pandharipande, R. W. Heath Jr. and I. B. Collings, "Adaptive MIMO Transmission for Exploiting the Capacity of Spatially Correlated Channels," accepted for publication in *IEEE Trans. on Veh. Tech.*, Apr. 2005.

[11] T. Svantesson and A. Ranheim, "Mutual Coupling Effects on the Capacity of Multielement Antenna Systems," in *Proc. IEEE Int. Conf. Acoust., Speech, and Sig. Proc.*, vol. 2, pp. 2485 2488, May 2001.

[12] X. Li and Z. P. Nie, "Mutual Coupling Effect on the Performance of MIMO Wireless Channels," *IEEE Ant. and Wireless Prop. Letters*, vol. 3, no. 1, pp. 344 - 347, 2004.

[13] C. Waldschmidt, S. Schulteis and W. Wiesbeck, "Complete RF System Model for Analysis of Compact MIMO Arrays," *IEEE Trans. on Veh. Tech.*, vol. 53, no. 3, pp. 579 - 586, May 2004.

[14] H. N. M. Mbonjo, J. Hansen and V. Hansen, "MIMO Capacity and Antenna Array Design," *IEEE Telecomm. Conf. Proc. Globecom*, vol. 5, pp. 3155 - 3159, Nov. 2004.

[15] J. W. Wallace and M. A. Jensen, "Mutual Coupling in MIMO Wireless Systems: A Rigorous Network Theory Analysis," *IEEE Trans. on Wireless Comm.*, vol. 3, no. 4, pp. 1317 - 1325, Jul. 2004.

[16] D. S. Shiu, G. J. Foschini, M. J. Gans and J. M. Kahn, "Fading Correlation and its Effect on the Capacity of Multielement Antenna Systems," *IEEE Trans. on Comm.*, vol. 48, no. 3, pp. 502 - 513, Mar. 2000.

[17] J. P. Kermoal, L. Schumacher, K. I. Pedersen, P. E. Mogensen and F. Frederiksen, "A Stochastic MIMO Radio Channel model with Experimental Validation," *IEEE Jrnl. on Select. Areas in Comm.*, vol. 20, no. 6, pp. 1211 - 1226, Aug. 2002.

[18] H. Ozcelik, M. Herdin, W. Weichselberger, J. Wallace and E. Bonek, "Deficiencies of Kronecker MIMO Radio Channel Model," *IEEE Elec. Letters*, vol. 39, no. 16, pp. 1209 1210, Aug. 2003.

[19] A. Forenza and R. W. Heath, Jr., "Benefit of Pattern Diversity Via 2-element Array of Circular Patch Antennas in Indoor Clustered MIMO Channels," *IEEE Trans. on Comm.*, vol. 54, no. 5, pp. 943 - 954, May 2006.

[20] K. Li, M. Ingram and A. Van Nguyen, "Impact of Clustering in Statistical Indoor Propagation Models on Link Capacity," *IEEE Trans. on Comm.*, vol. 50, no. 4, pp. 521 - 523, Apr. 2002.

[21] A. M. Saleh and R. A. Valenzuela, "A Statistical Model for Indoor Multipath Propagation," *IEEE Jour. Select. Areas in Comm.*, vol. SAC-5, no. 2, pp. 128 - 137, Feb. 1987.

[22] J. W. Wallace and M. A. Jensen, "Statistical Characteristics of Measured MIMO Wireless Channel Data and Comparison to Conventional Models," *Proc. IEEE Veh. Tech. Conf.*, vol. 2, no. 7 - 11, pp. 1078 - 1082, Oct. 2001.

[23] V. Erceg et.al., "TGn Channel Models," *IEEE 802.11-03/940r4*, http://www.802wirelessworld.com:8802/, May 2004.

[24] 3GPP Technical Specification Group, "Spatial channel model, SCM-134 text V6.0," *Spatial Channel Model AHG (Combined as-hoc from 3GPP and 3GPP2)*, Apr. 2003.

[25] D. Piazza and K. R Dandekar, "Reconfigurable Antenna Solution for MIMO-OFDM Systems," *IEE Elec. Letters*, vol. 42, no. 8, pp. 446 - 447, Apr. 2006.

[26] D. B. Davidson, I. P. Theron, U. Jakobus and F. M. Landstorfer, "Recent Progress on the Antenna Simulation Program FEKO,", *Proc. of COMSIG Conf.*, pp. 427 - 430, Sept. 1998.

[27] M. L. Morris and M. A. Jensen, "Network Model for MIMO Systems With Coupled Antennas and Noisy Amplifiers," *IEEE Trans. on Ant. and Prop.*, vol. 53, no. 1, pp. 545 - 552, Jan. 2005.

[28] A. Forenza and R. W. Heath, Jr., "Optimization Methodology for Designing 2-CPAs Exploiting Pattern Diversity in Clustered MIMO Channels," submitted to *IEEE Trans. on Comm.*, Jan. 2007.

[29] A. Forenza, G. Wan and R. W. Heath, Jr., "Optimization of 2-element Arrays of Circular Patch Antennas in Spatially Correlated MIMO Channels," *Proc. of the IEEE Int. Waveform Div. & Desn. Conf.*, Jan. 2006.

[30] D. Gore, R. W. Heath Jr., and A. Paulraj, "Transmit Selection om Spatial Multiplexing Systems," in *IEEE Comm. Lett.*, vol. 6, pp. 491 - 493, Nov. 2002.